MINISTRY OF EDUCATION AND TRAINING
VIETNAM ACADEMY OF SCIENCE AND TECHNOLOGY

GRADUATE UNIVERSITY OF SCIENCE AND TECHNOLOGY

PHAN KE SON

FABRICATION, CHEMO-THERMAL CANCER THERAPY EVALUATION AND *IN VIVO* DISTRIBUTION OF NEAR-INFRARED FLUORECENT MULTIFUNCTIONAL NANO DRUG DELIVERY SYSTEMS

SUMMARY OF DISSERTATION ON SCIENCES OF MATTER
Major: Polymer and Composite Materials
Code: 9440125

Hanoi - 2024

The dissertation is completed at: Graduate University of Science and Technology, Vietnam Academy Science and Technology.

Supervisors:

1. Supervisor 1: Assoc.Prof.Dr. Ha Phuong Thu
2. Supervisor 2: Dr. Le Thi Thu Huong

Referee 1: Assoc.Prof.Dr. Le Trong Lu

Referee 2: Assoc.Prof.Dr. Phan Minh Giang

Referee 3: Assoc.Prof.Dr. Duong Thi Ly Huong

The dissertation is examined by Examination Board of Graduate University of Science and Technology, Vietnam Academy of Science and Technology at 09:00 a.m. on September 28, 2024.

The dissertation can be found at:

1. Graduate University of Science and Technology Library
2. National Library of Vietnam

LIST OF THE PUBLICATIONS RELATED TO THE DISSERTATION

1. **Ke Son Phan**, Phuong Thu Ha*, Huu Nghi Do, Trung Anh Nguyen, Thuc Quang Bui, Hong Nam Pham, Mai Huong Le, Thi Thu Huong Le, "*Dual loading of Doxorubicin and magnetic iron oxide into PLA-TPGS nanoparticles: Design, in vitro drug release kinetics and biological effects on cancer cells*", **ChemMedChem**, 16, 2021, 3615–25 (SCIE, Q1, IF = 3.46).

2. **Ke Son Phan**, Bich Thuy DOAN,Thi Thu Huong Le, Thi Thu Trang Mai, Thi Dieu Thuy Ung, Thuc Quang Bui, Sarah Boumati, Phuong Thu Ha*, "*Near-Infrared Cyanine 5.5 and Doxorubicin loaded PLA-TPGS copolymer Based magnetite Nanoparticles for dual- in vivo Magnetic Resonance and Biodistribution Imaging*", **ChemistrySelect**, *8(40), e202303580, 2023* (SCIE, Q2, IF = 2.307).

3. **Phan Kế Sơn**, Lê Thị Thu Hương, Mai Thị Thu Trang, Đỗ Hữu Nghị, Bich Thuy DOAN, Phạm Hồng Nam, Nguyễn Hoài Nam, Đồng Thị Nhâm, Tô Xuân Thắng, Vương Thị Kim Oanh, Nguyễn Hải Bình, Hà Phương Thư*, "*Nghiên cứu chế tạo và đánh giá khả năng phân bố in vivo bằng hình ảnh huỳnh quang của hệ dẫn thuốc nano đa chức năng Fe_3O_4-Doxorubicin/Curcumin@PLA-TPGS-Cyanine 5.5*", The 12th National Conference on Solid State Physics & Materials Science 2022, p.859-864.

4. **Phan Kế Sơn**, Hà Phương Thư*, Lê Thị Thu Hương, Mai Thị Thu Trang, Đỗ Hữu Nghị, Bùi Thúc Quang, bằng độc quyền Sáng chế số 40854 "*Phương pháp sản xuất vật liệu nano đa chức năng trên nền copolyme PLA-TPGS mang đồng thời doxorubicin - nano oxit sắt từ*", được Cục Sở hữu trí tuệ cấp theo QĐ số 8527w/QĐ-SHTT ngày 17 tháng 7 năm 2024.

INTRODUCTION

1. The urgency of the PhD thesis

Currently, finding solutions to diagnose and effectively treat cancer is extremely necessary. Among cancer treatment methods, chemotherapy is still the most used method. However, traditional chemotherapy causes many side effects for patients, such as hair loss, weakness, reduced body immunity, diarrhea, nausea, etc. Therefore, attaching cancer treatment drugs to appropriate carrier systems that can deliver the drugs to the correct tumor location at the necessary dose is always a big challenge and needs to be solved by scientists. In addition to chemotherapy agents, magnetic iron oxide nanoparticles (Fe_3O_4 NPs) are widely used in cancer treatment due to their natural magnetic properties, targeting ability, ability to carry many biologically active substances, thermo-magnetic effect, and application as a contrast agent for magnetic resonance imaging (MRI).

Concurrently, cancer treatment is often a time-consuming process. When patients receive chemotherapy, they will often have to undergo additional tests to evaluate the effectiveness of the drug. One commonly used way to monitor cancer treatment is optical imaging techniques based on fluorescent substances. However, in *in vivo* observations of fluorescence or bioluminescence signals, due to optical characteristics such as absorption and scattering, deep tissue observation is very difficult. Near-infrared fluorophores have many advantages for biological processes compared to fluorescence in the visible spectrum, due to the lower autofluorescence and absorption of biological tissues in this wavelength region. Therefore, it facilitates the process of monitoring the *in vivo* distribution of drugs during treatment thanks to optical imaging.

From the above observation, it is shown that combining cancer chemotherapy drugs with Fe_3O_4 nanoparticles and near-infrared fluorescence can both help deliver anticancer drugs effectively to the tissue that needs treatment and monitor the treatment response of cancerous tissue. Combining such components is often accomplished using polymers. Although some previous studies have created a number of different multifunctional drug delivery systems, as far as we know, research combining these components has not been carried out.

The research in this PhD thesis designs a near-infrared fluorecent multifunctional nano drug delivery system PLA-TPGS-Fe_3O_4-Doxorubicin-Cyanine 5.5 attached. In particular, Doxorubicin's role as a chemotherapy drug is due to its ability to participate in many reactions and pathways that inhibit the growth of cancer cells. PLA-TPGS copolymer has the ability to

carry drugs thanks to the hydrophobic head and also has the ability to increase drug absorption thanks to the hydrophilic head, increasing treatment effectiveness and reducing the amount of drug needed. Nano-sized Fe_3O_4 plays a role in increasing the drug-carrying capacity of the system (the Fe_3O_4 nanosurface has a good adsorption capacity for Doxorubicin drug molecules). Besides, the Fe_3O_4 core with superparamagnetic properties (at a certain size) has the ability to self-heat under the influence of an external magnetic field. This allows the system to be applied to killing cancer cells using hyperthermia therapy.

Therefore, we decided to choose the topic of the PhD thesis as "**Fabrication, chemo-thermal cancer therapy evaluation and *in vivo* distribution of near-infrared fluorecent multifunctional nano drug delivery systems**". In this thesis, we fabricate a multifunctional nano drug delivery system based on Fe_3O_4 nanoparticles coated with PLA-TPGS copolymer, loading the drug Doxorubcin and attaching the near-infrared fluorescent agent Cyanine 5.5, with the following 4 new points:

(1) Monitoring the *in vivo* distribution of the multifunctional nano drug delivery system thanks to the near-infrared fluorescent capability of Cyanine 5.5. Through this, the ability to passively target the tumour's location and the organs' distribution characteristics in the *in vivo* model is assessed.

(2) Evaluating the chemotherapeutic effects of the multifunctional nano drug delivery system using the bioluminescence technique.

(3) The combination of chemotherapy and hyperthermia therapy produces outstanding tumour treatment. Concurrently, the mechanism of cancer cell poisoning of the multifunctional nano drug delivery system is determined by High Content Screening.

(4) In previous studies, in addition to determining the recovery of r_1 and r_2, the probability of increased contrast in MRI was determined by qualitative *in vivo* MR imaging. In this thesis, we quantified the MRI signal using the $\%I_{0.25}$ method to confirm the difference in the ability to increase contrast while demonstrating the passive targeting of the tumor location of the multifunctional nano drug delivery system on the CT26 colon tumor-causing mouse model.

2. The objectives

- Fabrication of multifunctional nanopharmaceutical conductors with near-infrared fluorescent agents.

- Evaluation of chemotherapeutic effects, ability to monitor and detect *in vivo* distribution of the drug in cancer tissues by near-infrared fluorescent agents, ability to increase contrast in nuclear resonance imaging, and hyperthermia capabilities of the multifunctional nano drug delivery systems.

3. The main research content

The main research content of the PhD thesis consists of 3 parts:

1. Research into the fabrication of the PLA-TPGS-Fe_3O_4-Doxorubicin NPs, characterization of physicochemical properties, drug release kinetics, toxicity assessment, and the cell toxic mechanism of the obtained nanosystem.

2. Research into the fabrication of the PLA-TPGS-Fe_3O_4-Doxorubicin-Cyanine 5.5 NPs, characterization of physicochemical properties, drug release kinetics, toxicity assessment, and the cell toxic mechanism of the obtained nanosystem.

3. Evaluation of the ability to increase contrast in MRI, *in vivo* distribution, chemotherapy, and hyperthemia of the near-infrared fluorescent multifunctional nanodrug delivery system PLA-TPGS-Fe_3O_4-Doxorubicin-Cyanine 5.5.

CHAPTER 1. OVERVIEW OF MULTIFUNCTIONAL NANO DRUG DELIVERY SYSTEM IN CANCER DIAGNOSIS AND TREATMENT

1.1. Overview of multifunctional nano drug delivery systems in cancer diagnosis and treatment

Current cancer treatments mainly include surgery, followed by radiotherapy and/or chemotherapy, and other new modalities such as immunotherapy, gene therapy, thermotherapy, and phototherapy. However, it is clear that, although successful to a certain extent, to date, such single modalities are unlikely to provide a complete treatment due to dose limitations and cellular drug resistance. cancer with this method. Therefore, if two or more of these methods can be combined on the same multifunctional system, it will help promote their advantages and avoid their disadvantages, and it is very possible to achieve the synergistic effect of 1 + 1 > 2. Among the cancer treatment methods mentioned above, chemotherapy is one of the most important therapies. Chemotherapy is effective against many types of cancer in practice. However, chemotherapy causes many side effects, which are due to a lack of targeting, drug resistance in cancer cells, and problems with the solubility, permeability, and stability of chemotherapy drugs. Therefore, drug delivery systems have been developed to limit these side effects. In addition, multifunctional drug delivery systems, combining anticancer drug delivery with other functions, have also been developed. However, it is also a challenge for two or more related functions to coordinate smoothly to maximize efficiency on the same nanomaterial. With the realization of these conditions, multifunctional nanomaterials are expected to be an effective cancer diagnosis and treatment therapy.

1.2. Polymers and polymer nanosystems

Polymers are compounds with long molecular chains and very large molecular masses due to the many chains (monomers) linked together by covalent bonds. Polymers have many applications in the development of multifunctional nanodrug delivery systems, which have brought about groundbreaking changes in the biomedical field. Nano-drug delivery systems using polymer or copolymer carriers can provide a sustainable, controlled, and targeted drug delivery method to improve treatment efficacy and reduce the side effects of traditional chemotherapy drugs. Polymers have many application advantages in nanodrug delivery systems, including (1) providing controlled drug release to the target site; (2) providing stability to unstable molecules (e.g., proteins, DNA, hydrophobic drugs, etc.); and (3) providing the possibility of modifying surfaces with binding media or receptors for the purpose of active targeted drug delivery.

Copolymers are polymers made of two or more different types of monomers, formed by polymerizing mixtures of monomers with different chemical structures. Among the copolymers, PLA-TPGS has attracted much attention in cancer drug delivery applications. PLA-TPGS copolymer is a type of amphiphilic copolymer used as a carrier in nanodrug delivery systems to increase cellular uptake thanks to its hydrophobic-hydrophilic balance and avoid rejection by the reticuloendothelial system. PLA-TPGS copolymer can be synthesized by ring-opening polymerization or simple conjugation of PLA with TPGS. The obtained copolymer can bring the special properties of TPGS to overcome the limitations of PLA and has been widely applied for anticancer drug delivery.

1.3. Fe_3O_4 coated polymer nano drug delivery system

Among potential applications, the application of Fe_3O_4 nanoparticles as a contrast-enhancing agent for nuclear magnetic resonance imaging (MRI) has soon been developed into a commercial product. MRI is a non-invasive imaging technique that uses the magnetic relaxation of water protons in the body to create three-dimensional tomographic images. To increase the stability and applicability of Fe_3O_4 nanoparticles, research has coated Fe_3O_4 with biocompatible polymers such as dextran, latex, polyethylene glycol, polyvinylpyrrolidone-iodine, poly(aspartic acid),... In addition, Fe_3O_4 nanoparticles have the potential to cause hyperthermia, increasing the temperature of the tumor area under the influence of an alternating magnetic field. To further enhance the effectiveness of multifunctional nanosystems, hyperthermia is often combined with chemotherapy. Furthermore, hyperthermia affects the fluidity and stability of cell membranes. It blocks the function of transmembrane proteins and cell surface receptors, thereby

facilitating nanoparticles to enter cells and increase their function. Therefore, combining the chemotherapeutic effect of anticancer drugs with the thermomagnetic effect of Fe_3O_4 increases drug toxicity due to improved drug absorption by cells and increased cell sensitivity to drugs.

However, one of the major challenges of multifunctional nanomaterials combined with chemo-thermotherapy for cancer is achieving homogeneous accumulation of the material in the tumor after injection. The therapeutic effect may be reduced due to the inhomogeneity of the thermal dose achieved within the tumor when a small amount of nanomaterials reaches the tumor site or due to the uneven distribution of nanomaterials within the tumor. Therefore, when designing multifunctional nanomaterials, it is necessary to further study their ability to penetrate and retain the tumor after injection. To achieve this purpose, near-infrared (NIR) fluorescence was used in the thesis research as a fluorescent tracer to monitor *in vivo* distribution and evaluate effectiveness. Tumor targeting of multifunctional nanomaterials.

1.4. Polymer nano drug delivery system attached to near-infrared fluorescence

The NIR fluorescence wavelength is useful for imaging applications and signal quantification in *in vivo* models. In recent years, many studies have developed effective methods to synthesize material systems carrying near-infrared fluorescence, and improve their optical properties for biological applications. Cyanine 5.5 has a maximum absorption/emission wavelength of 675/690 nm and was initially studied in *in vivo* optical imaging due to its low background noise. Applied to early cancer diagnosis, the research team of Choi and colleagues used Cyanine 5.5 as a fluorescent marker on the HT29 colon tumor mouse model. Cyanine 5.5 is conjugated to nanohyaluronic acid and poly(ethylene glycol), showing that the fluorescence signal concentrates in the tumor 1 hour after injection and continues to increase up to 6 hours after injection, then gradually decreases over time. Over time, tumor tissues are clearly distinguished from normal tissues, potentially for applications in early cancer diagnosis.

Review

Polymers and copolymers have many applications in the development of multifunctional nanodrug delivery systems, capable of overcoming many of the of the disadvantages of current medicinal chemicals. Nanodrug delivery systems have superior properties compared to traditional drugs, such as increased selective absorption and passive targeting, thanks to the effect of increasing storage permeability. Thereby reducing the toxicity and side effects of the drug and increasing the effectiveness of treatment. Fe3O4

nanoparticles have the potential to be used to increase the contrast of MRI images and exploit the thermomagnetic effect in cancer treatment when placed in an external magnetic field. Near-infrared fluorophores facilitate the monitoring of the *in vivo* distribution of drugs during treatment using optical imaging. The special feature of strong fluorescence in the near-infrared region is that it provides fluorescence images with little background scattering as well as the ability to penetrate deep tissue. Therefore, it is possible to create appropriate conditions for detecting and monitoring the biological processes of the drug delivery system, promising high efficiency in monitoring and treating cancer.

CHAPTER 2. MATERIALS AND METHODS

2.1. Synthesis of PLA–TPGS copolymer

PLA–TPGS copolymer was synthesized by ring-opening bulk polymerization of lactide monomer with vitamin E TPGS in the presence of stannous octoate as catalyst.

2.2. Synthesis of magnetic iron oxide nanoparticles (Fe_3O_4 NPs)

Magnetic iron oxide nanoparticles (Fe_3O_4 NPs) were synthesized by the co-precipitation method from Fe^{2+} and Fe^{3+} salts using the Sineo-Uwave 1000 microwave reactor system.

2.3. Synthesis of the multifunctional nano drug delivery system PLA-TPGS-Fe_3O_4-Doxorubicin

Dox and Fe_3O_4 NPs loaded nanoparticles based on PLA-TPGS copolymer were prepared by an emulsion solvent evaporation method.

2.4. Synthesis of the multifunctional nano drug delivery system PLA-TPGS-Fe_3O_4-Doxorubicin-Cyanine 5.5

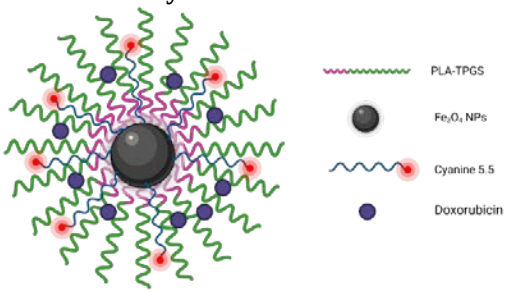

Fig. 2.1. Schematic illustration of the PLA-TPGS-Fe_3O_4-Cyanine 5.5-Doxorubicin nanosystem

Fe_3O_4 NPs were surface functionalized with 3-aminopropyltriethoxysilane (APTES), in the presence of EDC and NHS as catalysts, then encapsulated with Doxorubicin using PLA-TPGS copolymer (Fig. 2.1). Conditions such as ratio Fe_3O_4 : APTES (w/w), Cyanine 5.5 : Fe_3O_4 NPs (w/w), pH, temperature, and time of activation of Cyanine 5.5 were investigated.

2.5. Characterization of the nanoparticles

Fourier transform infrared spectroscopy (FTIR)
Field emission scanning electron microscopy (FESEM)
Transmission electron microscopy (TEM)
Thermogravimetric analysis (TGA)
Method for determining particle size distribution and zeta potential
Ultraviolet and visible absorption spectroscopy (UV-Vis)
Energy dispersive X-ray (XRD)
Vibrating sample magnetometer (VSM)
Magnetic inductive heating (MIH)

2.6. *In vitro* drug release studies

The drug-releasing kinetics of the PLA-TPGS-Fe_3O_4-Cyanine 5.5-Dox nanosystem have been investigated at simulated physiological condition (pH 7.4) and under simulated tumor extracellular matrix acidic conditions (pH 5.0 and 6.5) at 37 °C. In order to analysis of drug release from the nanosystem, six different kinetic models, i.e. Zero-Order, Higuchi, First-Order, Weibull, Hixson – crowell, and Korsmeyer-Peppas models were used.

2.7. Cell proliferation assay and mechanism of cancer cell toxicity

Cell viability was assessed through MTT [3-(4,5-dimethylthiazol-2-yl)-2,5-diphenyltetrazolium bromide] assay was adopted to measure the *in vitro* cytotoxicity of the nanoparticles in the cancer cell lines. A quantitative cytometric technique, the so-called high content screening (HCS) analysis, was used to define the cell cycle arrest of the effect of sample.

2.8. Evaluation of the ability to increase contrast in MRI

The MRI properties of selected nanoparticle systems were examined by measuring longitudinal T1 and transverse T2 protons relaxation times, using a 7 T MR imaging vertical spectrometer fitted with an ultra-shielded refrigerated magnet (300WB, Bruker, Avance II, Wissembourg, France). *In vivo* MRI signals on T2*-weighted MRI images (recorded in a FLASH sequence for effective T2 quantification) were quantified using the $\%I_{0,25}$ method.

2.9. Evaluation of the *in vivo* distribution of the NPs

The *in vivo* distribution of the NPs was evaluated by optical imaging on the CT26 rectal tumor mouse model using the Photon IMAGER Optima system, Biospace Lab, France.

2.10. Evaluation of chemotherapy effects using the bioluminescence technique

The chemotherapy effect of the NPs was evaluated through the level of luciferase gene expression in the tumor, based on the principle of the bioluminescence technique.

2.11. *In vivo* hyperthermia experiment

The mice were injected directly into the tumor with nanomaterials at a dose of 150 µL/mouse. Then, 40 minutes later, a hyperthermia test was conducted to ensure particle dispersion within the tumor. An AC magnetic field was applied four times, each time 72 hours apart, on the RDO, model HFI (Institute of Materials Science), with an intensity of 150 Oe and a frequency of 450 kHz, for a period of 30 minutes. The weight, size, and image of the tumor were recorded just before treatment to evaluate the effect of hyperthermia on tumor growth as well as the mouse's physical condition.

CHAPTER 3. THE MULTIFUNCTIONAL NANO DRUG DELIVERY SYSTEM PLA-TPGS-Fe_3O_4-DOXORUBICIN

3.1. Synthesis of PLA-TPGS copolymer

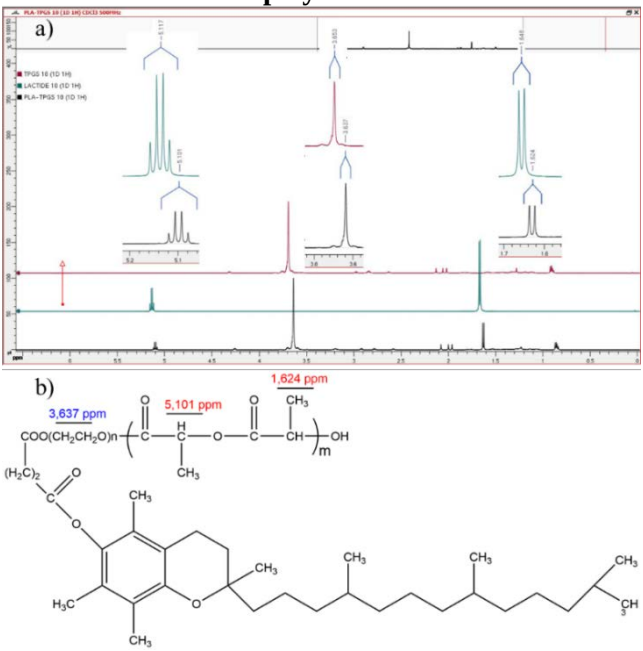

Fig. 3.1. (a) ^{1}H-NMR spectra of lactide, TPGS and PLA-TPGS copolymer, (b) molecular structure of PLA-TPGS copolymer

The structure of the synthesized PLA-TPGS copolymer was detected by ^{1}H-NMR in $CDCl_3$ (Fig. 3.1). The signals at 5.117 and 1.646 ppm were assigned to the -CH protons and methyl protons -CH_3 of the PLA segment, respectively. The signal at 3.653 ppm of the spectrum of TPGS was assigned to the –CH_2CH_2– protons. These three peaks were, correspondingly, shifted to 5.101, 1.624, and 3.637 ppm in the spectrum of the PLA-TPGS copolymer. This observation shows that PLA-TPGS was successfully

synthesized and purified. The molecular structure of PLA-TPGS copolymer is presented in Fig. 3.1b.

3.2. Synthesis of the multi-functional nano drug delivery system PLA-TPGS-Fe_3O_4-Doxorubicin

The multifunctional nano drug delivery system co-loading Fe_3O_4 NPs and Doxorubicin (PLA-TPGS-Fe_3O_4-Doxorubicin, MNDDS) with Dox : Fe_3O_4 NPs w/w = 1:1 ratio is optimal in terms of size, durability, durability, loading capacity and encapsulation efficiency of Doxorubicin (Table 3.1).

Table 3.1. Optimization of loading ratio between Dox and Fe_3O_4 NPs (n=3, mean ± SD)

Samples	Dox: Fe_3O_4 NPs ratio (w/w)	Size (nm)	Polydispersity index (PDI)	Zeta potential in distilled water (mV)	Zeta potential in PBS buffer (mV)	Dox loading (%)	Entrapment Efficiency (%)
MNDDS1	1 : 5	217.47 ± 4.78	0.190 ± 0.009	-28.7 ± 0.9	-17.5 ± 1.1	7.97 ± 0.33	86.49 ± 0.36
MNDDS2	2 : 5	172.33 ± 2.05	0.411 ± 0.041	-22.6 ± 1.0	-19.3 ± 0.8	13.44 ± 0.38	77.67 ± 0.90
MNDDS3	1 : 2	167.60 ± 2.62	0.394 ± 0.012	-29.6 ± 1.3	-21.1 ± 1.5	18.13 ± 0.78	88.64 ± 0.45
MNDDS4	1: 1	147.50 ± 1.22	0.146 ± 0.007	-41.1 ± 0.9	-28.4 ± 1.3	31.28 ± 1.64	91.05 ± 0.85
MNDDS5	2 : 1	288.67 ± 1.25	0.371 ± 0.005	-30.8 ± 1.3	-23.9 ± 1.4	44.29 ± 1.03	79.52 ± 1.36

3.3. Physicochemical properties

The MNDDS micelles have spherical shape with a uniform diameter of about 20 nm (Fig. 3.2a). In the transmission electron microscopy (TEM) image, the MNDDS appeared as nearly spherical shape at the size range from 17.0 to 19.8 nm (Fig. 3.2b). Characteristic X-ray diffraction (XRD) peaks (Fig. 3.3) for Fe_3O_4 NPs were found at $2\theta = 30.74°$, 35.86°, 43.38°, 54.04°, 57.3°, and 63.02°, fitting to (220), (311), (400), (422), (511) and (440) planes which were characteristic for single phase spinel structure of Fe_3O_4 nanoparticles. The presence of PLA-TPGS copolymer and Doxorubicin in the MNDDS only caused the low-intensity peaks but no difference in position compared with that of bare Fe_3O_4 nanoparticles. Therefore, Fe_3O_4 NPs in the MNDDS sample remained their crystal structure during the encapsulation procedure. The calculated mean crystalline size of the Fe_3O_4 NPs and the MNDDS sample through the Scherrer formula were about 11.55 nm and 10.72 nm, respectively.

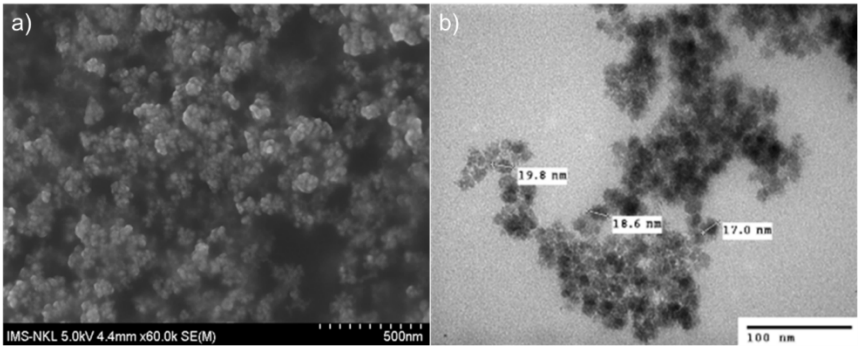

Fig. 3.2. (a) FESEM image, (b) TEM image of the PLA-TPGS-Fe_3O_4-Doxorubicin NPs

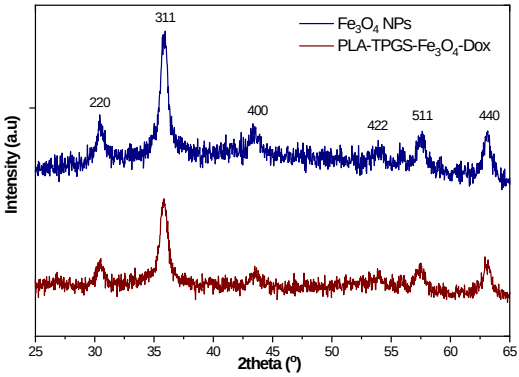

Fig. 3.3. The X-ray diffraction pattern (XRD) of Fe_3O_4 NPs and PLA-TPGS-Fe_3O_4-Doxorubicin NPs

The magnetization at 11 kOe of Fe_3O_4 NPs was 66.1 emu/g. This value of MNDDS nanoparticles was reduced compared to Fe_3O_4 NPs due to the encapsulation of Fe_3O_4 NPs by the PLA-TPGS copolymer and the effect of Dox when co-loaded on the nanosystems. All 5 MNDDS samples showed heat-generating possibilities for cancer therapy application (reaching the T_{max} region> 50^oC at 1500s) at 100 Oe/340 kHz. Tumor cells typically have a higher thermal sensitivity than normal cells at about 43°C, leading to tumor cell damage. This again showed the potentiality of the MNDDS samples in the hyperthermia treatment.

3.4. *In vitro* drug release kinetics and mechanism of release

Preliminary analysis of the in *vitro* release of Dox from the MNDDS nanoparticles indicated that a sustained release behavior and strong

dependence on the pH of the medium, compared to the release pattern of free Dox. More than 95% of free Dox was released massively after the first hour in both pH environments. By contrast, the Dox release from the nanoparticles displayed a biphasic release profile. The initial burst associated with the fast release of drug molecules took place in the first 12 h while the second phase was sustainable release in the next hours. Otherwise, Doxorubicin's *in vitro* drug release kinetics from this nanosystem was best fitted to the Weibull kinetic model. Under acidic pH conditions, Dox was released from the nanosystem by the classical Fickian diffusion mechanism, Dox was released at physiological pH by the simultaneous action of swelling and erosion mechanisms of PLA-TPGS copolymer.

3.5. *In vitro* cytotoxicity

All five MNDDS nanosystems had high cytotoxic activity with low IC_{50} values of less than 2 μg mL^{-1} (Fig. 3.4). Most of the MNDDS nanosystems showed lower IC_{50} values than free Dox, except for MNDDS3 on HeLa, HGC-27 and PC3 cell lines. Besides, a remarkable difference in IC_{50} value between free Dox and MNDDS samples was shown on CCF-STTG1 cell line ($p<0.001$). These results suggest that the MNDDSs could be a good candidate for human brain tumor treatment.

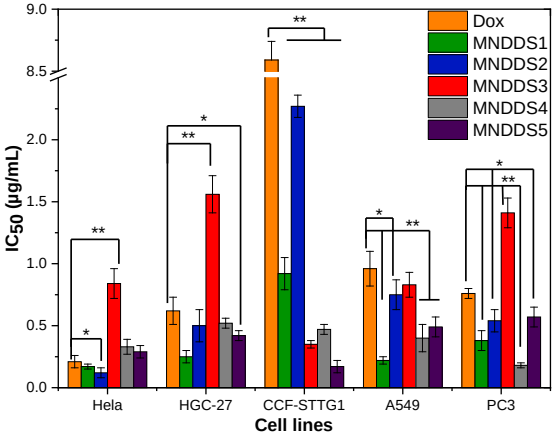

Fig. 3.4. *In vitro* cytotoxicity evaluation of free Dox and the MNDDS samples (***p<0.001; and *p<0.05* (n=3) versus control*)*

To assess the cancer toxicity mechanism of Nano Pla-TPGS-FE3O4-Doxorubicin system, the capture of cell cycles is assessed by high-hearted screening techniques (HCS). The cell cycle distribution in G0/G1 phase of free Dox-treated HeLa cells was 28.68%, while the figure for control group was 62.46%. The MNDDSs with different Dox: Fe_3O_4 NPs ratios result in various changes in cell cycle profile. There was an increase in the cell

population in G0/G1 phase of MNDDS1-treated sample compared to control. Meanwhile, for the remaining 4 MNDDSs, more cells in G2/M than control were observed.

CHAPTER 4. THE NEAR-INFRARED FLUORECENT MULTIFUNCTIONAL NANO DRUG DELIVERY SYSTEM PLA-TPGS-Fe_3O_4-Doxorubicin-Cyanine 5.5

4.1. Optimization of PLA-TPGS-Fe_3O_4-Doxorubicin-Cyanine 5.5 NPs

The PLA-TPGS-Fe_3O_4-Dox-Cyanine 5.5 NPs had good fluorescence ability, with the following optimal conditions including Fe_3O_4 NPs : APTES (w/w) ratio= 10 : 3; Cyanine 5.5 : Fe_3O_4 NPs (w/w) ratio = 0,05 : 1; temperature 70 ^oC; pH 8.5; 5 hour reaction time (Fig. 4.1).

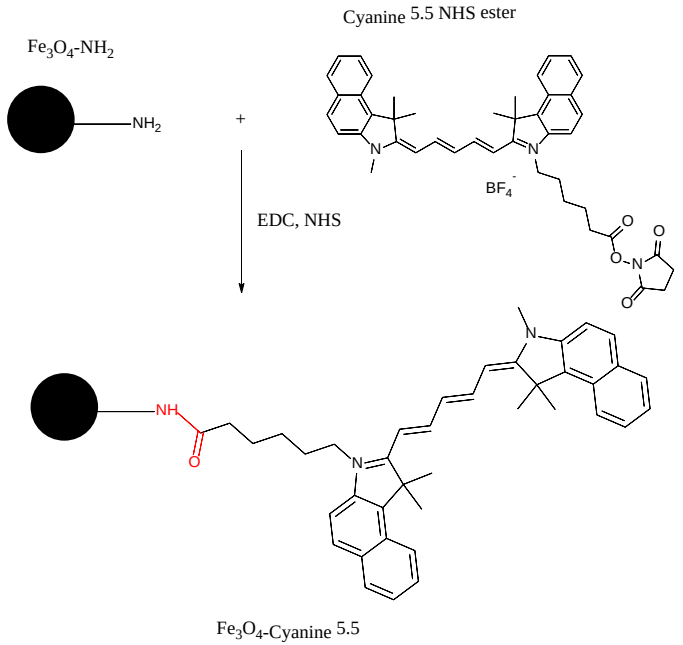

Fig. 4.1. Reaction diagram of attaching Cyanine 5.5 to the Fe_3O_4-NH_2 surface

4.2. Physicochemical properties

As shown in Fig. 4.2a, the main emission peaks at approximately 716 nm and 594 nm corresponding to Cyanine 5.5 and Dox free were observed. After loading Cyanine 5.5, the emission of PLA-TPGS-Fe_3O_4-Cyanine 5.5 nanosystem was 6-nm redshifted in comparison to free Cyanine 5.5. The redshift can be explained by the increase in nanoparticle size and/or the

interaction between iron oxide nanoparticles and attached Cyanine 5.5 encapsulated in the PLA-TPGS copolymer. Meanwhile, a blue-shift in the PLA-TPGS-Fe_3O_4-Cyanine 5.5-Dox spectrum could be due to the interaction between Dox and the other components in the nanosystems. As a result of these interactions, the luminescence intensity of both PLA-TPGS-Fe_3O_4-Cyanine 5.5 and PLA-TPGS-Fe_3O_4-Cyanine 5.5-Dox samples was lower than that of Cyanine 5.5 and Dox free. Moreover, the lower emission intensity was attributed to the quenching of the fluorescent entity by the Fe_3O_4 NPs core.

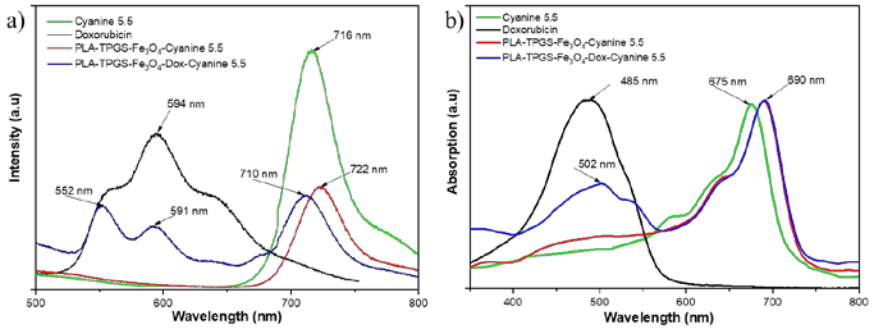

Fig. 4.2. (a) Fluorescent spectroscopy and (b) UV−vis spectroscopy of PLA-TPGS-Fe_3O_4-Cyanine 5.5-Dox NPs and ingredients

The UV absorption spectra of the nanoparticles before and after loading with Cyanine 5.5 and Doxorubicin are presented in Fig. 4.2b. Cyanine 5.5 free displayed a typical absorption band at 675 nm. Interestingly, the absorption of both the PLA-TPGS-Fe_3O_4-Cyanine 5.5 and PLA-TPGS-Fe_3O_4-Cyanine 5.5-Dox nanoparticles was recorded in the near-infrared region with a redshift of 15 nm from 675 to 690 nm. The redshift in the absorption spectrum of nanoparticles might be explained by the formation of the NH-CO bond between Cyanine 5.5 molecule and the Fe_3O_4 NPs surface, which places the Cyanine 5.5 molecule in a more hydrophobic environment by hydrophobic nature of Fe_3O_4 NPs and PLA chains of the PLA-TPGS copolymer.

Fig. 4.3 shows the TEM image of the PLA-TPGS-Fe_3O_4-Cyanine 5.5 and PLA-TPGS-Fe_3O_4-Cyanine 5.5-Dox samples. It can be seen that the nanoparticles are spherical and mono-dispersed without large aggregation. The particle size was about 10 - 15 nm with narrow size distrubution. The average size of the PLA-TPGS-Fe_3O_4-Cyanine 5.5 and PLA-TPGS-Fe_3O_4-

Cyanine 5.5-Dox nanoparticles measured from TEM images by ImageJ were 12.19 ± 1.81 nm and 13.16 ± 2.16 nm, respectively.

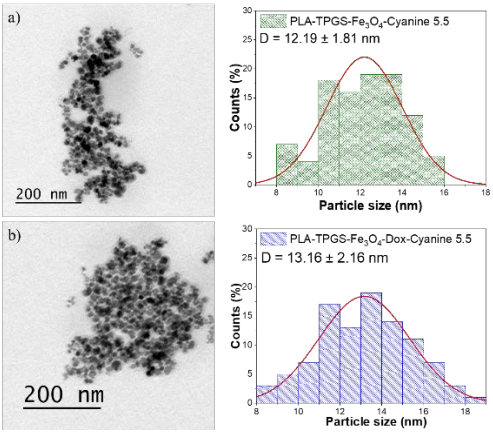

Fig. 4.3. TEM images and histogram of size distribution of (a) PLA-TPGS-Fe_3O_4-Cyanine 5.5; (b) PLA-TPGS-Fe_3O_4-Cyanine 5.5-Dox NPs

From the patterns, Fig. 4.4a shows that prominent peaks observed at 30.34° (220), 35.71° (311), 43.22° (400), 53.65° (422), 57.24° (511), and 63.09° (440) are in good accordance with the inverse cubic spinel phase of Fe_3O_4 (magnetite, JCPDS card no. 85-1436). The XRD patterns of the PLA-TPGS-Fe_3O_4-Cyanine 5.5 and PLA-TPGS-Fe_3O_4-Cyanine 5.5-Dox nanoparticles showed no shifting in position but broadened characteristic peaks, indicating the successful encapsulation of APTES and PLA-TPGS copolymer, the loading of Cyanine 5.5 and Doxorubicin without degrading the core magnetite. This result leads to the preservation of the magnetic properties of the nanosystem, which can be clearly seen in subsequent research results.

The saturation magnetization (M_S) was around 67.4 emu/g for the bare Fe_3O_4 NPs at 300 K. However, the saturation magnetization of the coated nanoparticle was significantly reduced (Fig. 4.4b). It is observed that the saturation magnetic moment values for the PLA-TPGS-Fe_3O_4-Cyanine 5.5 and PLA-TPGS-Fe_3O_4-Cyanine 5.5-Dox NPs were found to be 54.6 and 38.6 emu/g, respectively. The low M_S value of both nanosystems is due to the diamagnetic contribution of Cyanine 5.5, Doxorubicin, and PLA-TPGS copolymer of the organic shell.

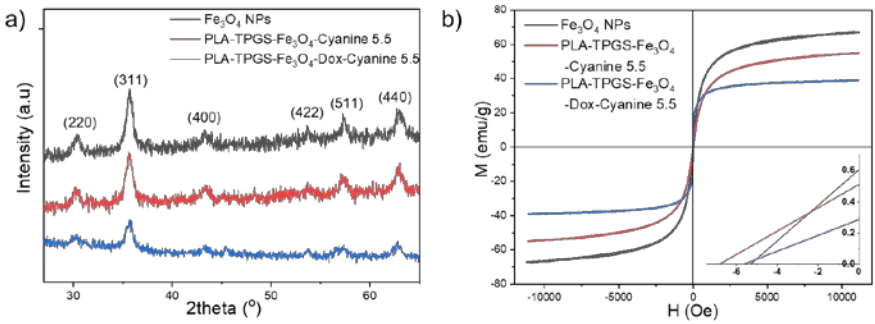

Fig. 4.4. (a) XRD patterns and (b) the hysteresis loops of pure Fe_3O_4 NPs PLA-TPGS-Fe_3O_4-Cyanine 5.5 and PLA-TPGS-Fe_3O_4-Cyanine 5.5-Dox measured at 300 K.

4.3. *In vitro* release study

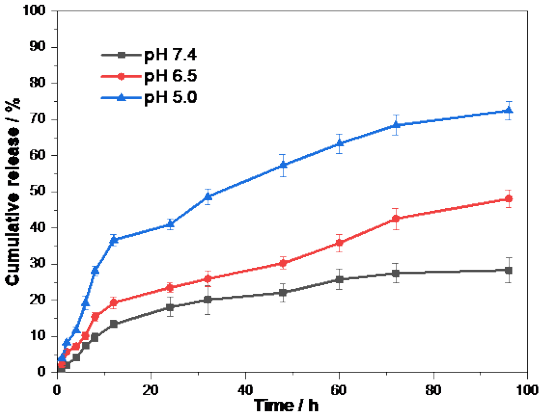

Fig. 4.5. *In vitro* drug release profiles of Doxorubicin from the nanosystems in pH 7.4, 6.5, and 5.0 solutions

The drug release kinetics clearly reveal pH dependent Dox release from this nanosystem (Fig. 4.5). The Dox release at physiological pH was observed to be slow, with an initial approximately 9% release during the the first 8 hours and only 28.33% release in 96 h. The drug release rate increased as the pH value decreased. The drug release rate at pH 5.0 and 6.5 increased more obviously than that at pH 7.4. The cumulative drug release was about 48% at pH 6.5 within 96 h, and it increased to 72.47% at pH 5.0. This finding infers that most Dox encapsulated with PLA-TPGS copolymer will remain intact in the plasma (pH 7.4) after injection, considerably reducing the possibility of systemic adverse effects on healthy tissues. By contrast, faster

Dox release will occur after the nanosystem penetrates the tumor, because of a much lower pH (5.0 to 6.5) than physiological pH.

4.4. *In vitro* cytotoxicity

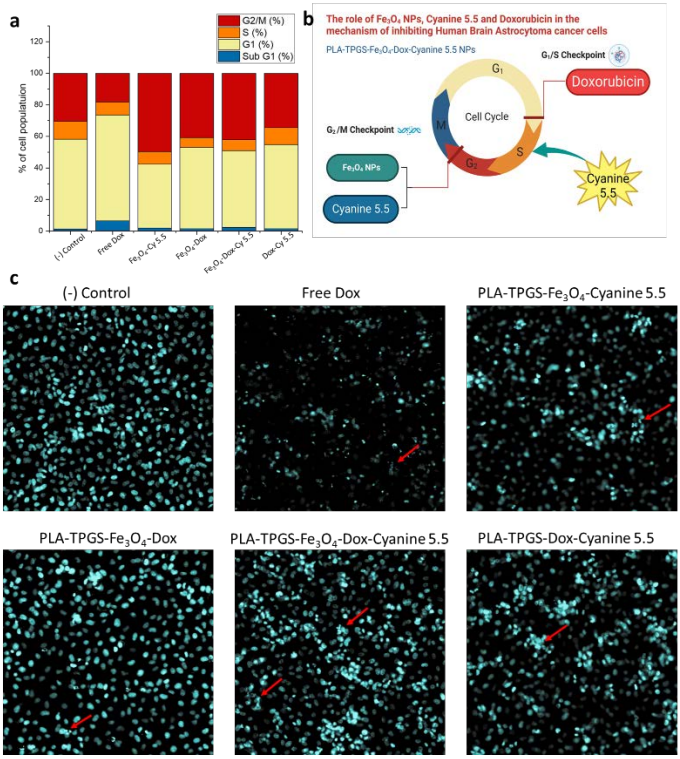

Fig. 4.6. (a) Cell cycle distribution in CCF-SSTG1 cells; (b) Schematic illustration of the cytotoxic mechanism; (c) Confocal imaging four NPs for CCF-SSTG1 cells (20x magnification, sCMOS camera). *The red arrow showed cells induced to undergo apoptosis.*

Cell cycle analysis results have once again confirmed the cytotoxic role of Fe_3O_4 NPs, Dox, and Cyanine 5.5 in nanosystems by a quantitative cytometric technique, the so-called high content screening (HCS) analysis. Fig. 4.6a showed that free Dox arrested cell cycle progression in the G1 phase of human brain astrocytoma cells by 67.02%. The combination of Cyanine 5.5 and Dox in the PLA-TPGS-Dox-Cyanine 5.5 NPs reduced the cell population in the G1 phase to 53.23% and slightly increased the cell population in the G2/M phase to 34.44%. By contrast, the cell cycle distribution in the G2/M phase of CCF-STTG1 cells treated with PLA-TPGS-Fe_3O_4-Cyanine 5.5 was 49.69%, while the figure for the negative

control group was 30.5% (Fig. S2). Compared to the control group, the PLA-TPGS-Fe_3O_4-Dox-Cyanine 5.5 nanosystem increased the percentage of cells in the G2/M phase higher than the PLA-TPGS-Fe_3O_4-Dox system, 42.12% and 40.79%, respectively. Thus, the results demonstrated that Fe_3O_4 and Cyanine 5.5 present a cytostatic effect, inducing cell cycle arrest at the G2/M phase for human brain astrocytoma cells. Fig. 4.6c showed that all NPs induced apoptosis in CCF-STTG1 cells (red arrow), indicating the presence of dead cells.

CHAPTER 5. EVALUATION OF THE ABILITY TO INCREASE CONTRAST IN NUCLEAR MAGNETIC RESONANCE IMAGING, *IN VIVO* DISTRIBUTION, CHEMOTHERAPY AND MAGNETIC THERMAL EFFECTS OF THE NEAR-INFRARED FLUORECENT MULTIFUNCTIONAL NANO DRUG DELIVERY SYSTEMS

5.1. Evaluation of the ability to increase contrast in MRI

Another important role of Fe_3O_4 NPs is its use as a potential MR imaging contrast agents. One key question with this strategy is whether Dox and Cyanine 5.5, which were loaded into the Fe_3O_4-encapsulated PLA-TPGS NPs, can effectively relax the surrounding water molecules and provide sufficient imaging contrast. In theory, the Fe_3O_4-encapsulated PLA-TPGS NPs need to be an efficient interchange of water or the polymeric components to be a successful relaxation agent. Therefore, the MRI contrast enhancement effects of the Fe_3O_4 NPs and the magnetite-based nanosystems with or without Dox and Cyanine 5.5 were evaluated on a 7T MR imaging vertical spectrometer at room temperature.

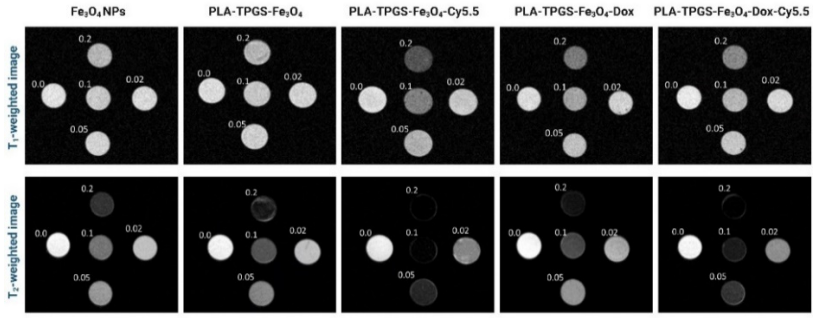

Fig. 5.1. T1-weighted and T2-weighted MR images of Fe_3O_4 NPs; PLA-TPGS-Fe_3O_4; PLA-TPGS-Fe_3O_4-Cyanine 5.5; PLA-TPGS-Fe_3O_4-Dox; PLA-TPGS-Fe_3O_4-Dox-Cyanine 5.5 and PLA-TPGS-Dox-Cyanine 5.5 NPs

Fig. 5.1 is the magnetic resonance image of the Fe_3O_4 NPs, PLA-TPGS-Fe_3O_4, Fe_3O_4-Cyanine 5.5, PLA-TPGS-Fe_3O_4-Dox, and PLA -TPGS

-Fe_3O_4-Dox-Cyanine 5.5 various concentrations of 0.02 mM, 0.05 mM and 0.1 mM (calculated for element Fe) in T1-weighted (left), T2-weighted (right) images. It can be seen that the dark signal gradually increases with Fe concentration in the nanosystems present in the wells compared to the 1% agarose control (well 0). Table 5.1 shows that the experimentally determined r_2/r_1 ratio followed an order of PLA-TPGS-Fe_3O_4-Dox-Cyanine 5.5 (375.9) > PLA-TPGS-Fe_3O_4-Cyanine 5.5 (325.4) > PLA-TPGS-Fe_3O_4-Dox (302.1). The mechanism behind the contrast enhancement of Cyanine 5.5 and Doxorubicin was further proposed in Fig. 5.2. These findings suggest that the chemical structure of Cyanine 5.5 and Doxorubicin significantly contributes to the enhancement of the T_2 relaxivities of Fe_3O_4 NPs.

Table 5.1. MRI relaxivivty (s^{-1} mM^{-1}) and r_2/r_1 ratios at 7 T of NPs

Sample	r_2 (s^{-1} mM^{-1})	r_1 (s^{-1} mM^{-1})	r_2/r_1
Fe_3O_4 NPs	198,88	0,9725	204,5
PLA-TPGS-Fe_3O_4	237,13	0,8717	272,0
PLA-TPGS-Fe_3O_4-Cyanine 5.5	249,92	0,768	325,4
PLA-TPGS-Fe_3O_4-Dox	282,21	0,9343	302,1
PLA-TPGS-Fe_3O_4-Dox-Cyanine 5.5	305,83	0,8135	375,9

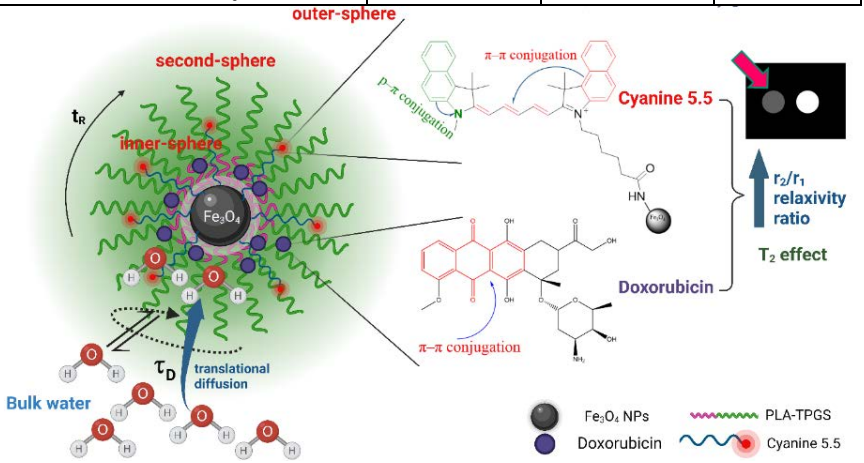

Fig. 5.2. Schematic illustration of the enhanced contrast mechanism of Cyanine 5.5 and Doxorubicin

In this thesis, in addition to evaluating *in vivo* MRI imaging, we further analyze the effectiveness of passive targeting in CT26 colon tumors by quantifying the signal on T2*-weighted MRI images, using the $\%I_{0.25}$ processing method. Regions of interest (ROIs) were drawn on each slice of the tumor on the MRI image (Fig. 5.3a, c), and the pixel intensity distribution for each slice was obtained. Aggregating these pixel intensity distribution

plots gives a unique pixel intensity distribution for each tumor, as shown in Fig. 5.3b,d. Fig. 5.3e shows that the percentage of pixels below I0.25 has a significant difference ($p<0.001$) between uninjected mice and mice 4 hours after nanomaterial injection, 3.35 and 13.82%, respectively. This reflects the effective passive accumulation of nanomaterials in these tumors.

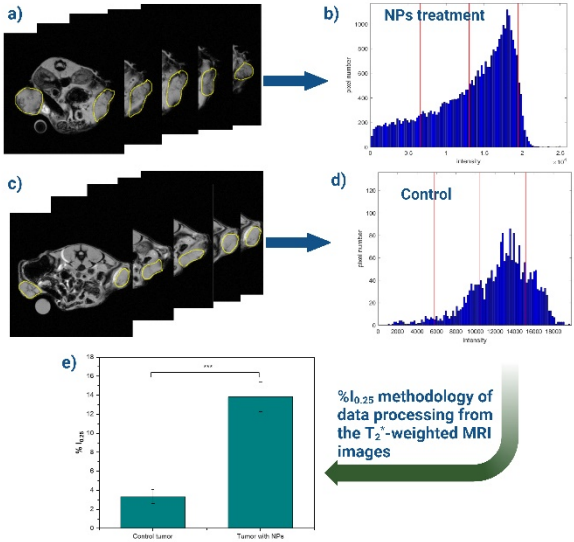

Fig. 5.3. The $\%I_{0.25}$ method processes data from T2*-weighted MRI images to evaluate the *in vivo* accumulation of PLA-TPGS-Fe_3O_4-Dox-Cyanine 5.5 nanosystems in tumors. a) MRI image in mice 4 hours after injection; b) MRI intensity distribution related to the tumor 4 hours after injection; c) MRI images in control mice; d) Tumor-related MRI intensity distribution in control mice; e) Summary of percentage of pixels below $\%I_{0.25}$ on MRI tumor images. Mann-Whitney test for non-gaussian distribution: *p < 0,05; **p < 0,01; *** p < 0,001.

5.2. Evaluation of *in vivo* distribution using the bioimaging technique

To study the *in vivo* biodistribution of the near-infrared fluorecent multifunctional nano drug delivery system, mice bearing CT26 tumor were injected into the eye vein (Fig. 5.4a) with 150 µL of PLA-TPGS-Fe_3O_4-Dox-Cyanine 5.5 (equivalent to 0.065 mM Cyanine 5.5). Fig. 5.4b depicts the *in vivo* distribution over time of the PLA-TPGS-Fe3O4-Dox-Cyanine 5.5 nanosystem at the following time points: 5 minutes, 15 minutes, 30 minutes, 1 hour, 3 hours, 6 hours, and 24 hours after injection. Fluorescent signals were analyzed using M3 vision software (BioSpace Lab, France) and expressed as average radiance (ph/s/cm^2/sr).

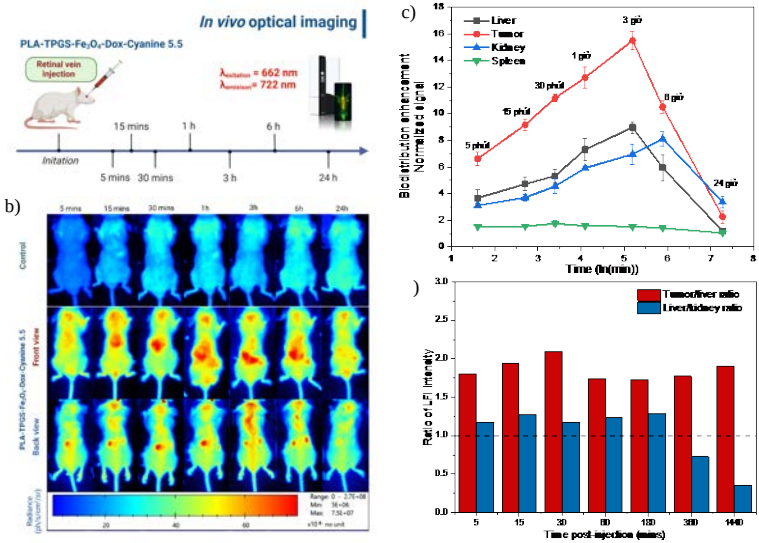

Fig. 5.4. (a) Schedule of *in vivo* experimental setup; (b) *in vivo* distribution over time of the PLA-TPGS-Fe_3O_4-Dox-Cyanie 5.5 NPs on a CT26 tumor-bearing mouse model; (c) quantification of fluorescence signals in tumors and organs of mice; and (d) tumor/liver and liver/kidney signal ratios.

Immediately after 5 minutes of injection, fluorescence signals began to be observed, highest in the tumor, followed by the liver, kidney, and spleen (Fig. 5.4c). Fluorescence intensity in the tumor, liver, and kidney gradually increased over time. After 3 hours of injection, the signal was highest in the tumor, followed by the liver. This result is also compatible with the quantitative MRI results above, showing the effectiveness of passive targeting to the tumor site of the multifunctional nanosystem PLA-TPGS-Fe_3O_4-Dox-Cyanine 5.5. Concurrently, the high fluorescence signal in the liver showed that part of the nanosystem had accumulated in the liver, which is the organ responsible for removing foreign objects from the circulatory system.

Interestingly, the fluorescence signal in the kidney was highest at 6 hours. After 24 hours, the fluorescence signal in the tumor was low and clearly reduced (5.6 times compared to 3 hours), but the fluorescence intensity was highest in the mouse kidney, followed by the liver and spleen. This result shows that this nanosystem has begun to be eliminated from the body and that the NPs' survival time in the body is at least 24 hours. Finally, the fluorescence signal in the spleen was very low, not changing significantly over the 24-hour period. These results demonstrate that the PLA-TPGS-Fe_3O_4-Dox-Cyanine 5.5 nanosystem is a promising multifunctional

nanodrug delivery system for *in vivo* NIR biodistribution imaging applications in biomedicine.

5.3. Evaluation of chemotherapy effects using the bioluminescence technique

In this PhD thesis, we use luciferase bioluminescence imaging to evaluate the tumor response to the chemotherapy effects of the multifunctional nano drug delivery system PLA-TPGS-Fe3O4-Dox-Cyanine 5.5. Because the luciferase gene is inserted into the CT26 tumor marker gene, they will always be expressed together. Therefore, after luciferin injection, a bioluminescent signal is generated only in cancer cells at the tumor site due to luciferase activity. The intensity of the bioluminescent signal allows assessing the viability of cancer cells (Fig. 5.5). In mice injected with PLA-TPGS-Fe_3O_4-Dox-Cyanine 5.5, the fluorescence signal decreased rapidly after 72 hours, indicating a loss of luciferase activity. In contrast, the bioluminescence intensity in mice injected with PLA-TPGS-Fe_3O_4-Cyanine 5.5 was not significantly reduced compared to the control group injected with PBS solution (the difference was not statistically significant, $p > 0.05$). This proves that the chemotherapy effect of the multifunctional nano drug delivery system PLA-TPGS-Fe_3O_4-Dox-Cyanine 5.5 effectively inhibits tumor growth, with the effect clearly visible after 72 hours of injection.

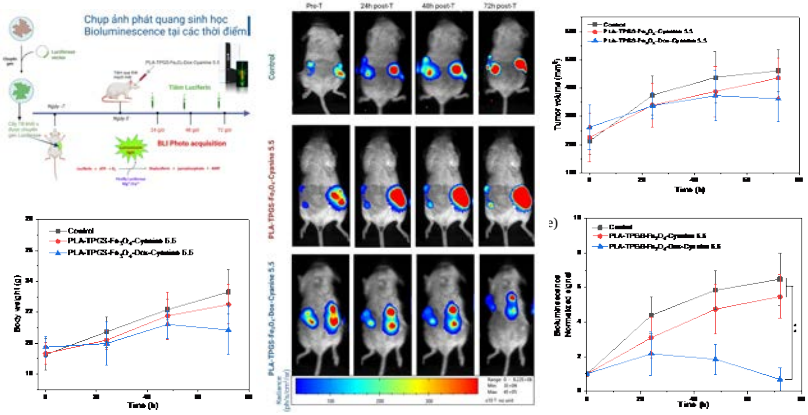

Fig. 5.5. Evaluation of the chemotherapy effects of PLA-TPGS-Fe_3O_4-Dox-Cyanine 5.5 NPs using bioluminescence imaging. (a) Experimental diagram; (b) body weight; (c) representative mice of each experimental group show luciferase activity in the tumor; (d) tumor volume; (e) average luciferase activity in tumors with standard deviation. The luciferase signal was normalized with the signal before treatment.

5.4. Hyperthermia effect

After 4 treatments, the tumor size in the group (PLA-TPGS-Fe_3O_4-Dox-Cyanine 5.5 injection + magnetic field irradiation) was clearly different from the control group. The tumor volume reached 3077 ± 280 mm3, significantly different from the negative control group ($p < 0.001$) and the remaining groups ($p < 0.05$). This result shows a synergistic effect when combining chemotherapy (Dox) with hyperthermia therapy (Fe_3O_4 + magnetic field irradiation) in the LA-TPGS-Fe_3O_4-Dox-Cyanine 5.5 NPs (Fig. 5.6). Along with previous results, this study's results once again confirm that the magnetothermic method using Fe_3O_4 nanoparticles combined with the chemotherapy effect of Doxorubicin is a promising method in cancer treatment.

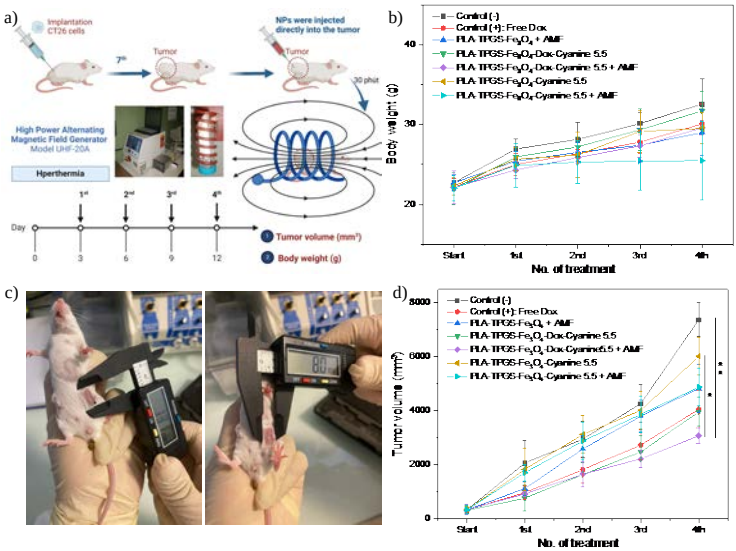

Fig. 5.6. (a) Experimental diagram to evaluate the *in vivo* hyperthermia effect; (b) mouse mass monitoring; (c) measure tumor size in mice; (d) tumor volume (*$p < 0.05$; **$p < 0.001$)

CONCLUSIONS AND RECOMMENDATIONS

The PhD thesis has focused on researching and fabricating the near-infrared fluorescent multifunctional nano drug delivery systems based on PLA-TPGS copolymer. In particular, the PLA-TPGS-Fe_3O_4-Doxorubicin-Cyanine 5.5 nanosystem includes the following functions: (1) loading Doxorubicin; (2) enhancing MRI image contrast; (3) chemotherapy effect of Doxorubicin; (4) hyperthermia effects; and (5) monitoring *in vivo* distribution and treatment effectiveness using optical imaging techniques.

From the detailed research results and appropriate discussions, some main conclusions are drawn as follows:

1. A multifunctional nanosystem co-loading Doxorubicin and Fe_3O_4 has been fabricated and characterized, in which the ratio of Dox to Fe_3O_4 NPs is 1 : 1 w/w. The obtained PLA-TPGS-Fe_3O_4-Dox nanosystem has a spherical shape, an average particle size of 17–19.8 nm, an encapsulation efficiency of 91.05 ± 0.8%, and a and a loading capacity of Doxorubicin of 31.28 ± 1.64 %. *In vitro* drug release kinetics of Doxorubicin from this nanosystem fitted best to the Weibull kinetic model and the drug release mechanism depends on pH. The PLA-TPGS-Fe_3O_4-Doxorubicin nanosystem has an effective cytotoxic effect on cancer cells, has the ability to penetrate cells, and has the potential to be applied in hyperthermia therapy. On the HeLa cervical cancer cell line, the nanosystem has a high Fe_3O_4 ratio, causing cytotoxicity by arresting cells in the G0/G1 phase. Meanwhile, nanosystems with a higher proportion of Doxorubicin will cause cytotoxicity by arresting cells in the G2/M phase.

2. A near-infrared fluorescent multifunctional nano drug delivery system has been fabricated and characterized with the following technical parameters: with the following technical parameters: ratio Cyanine 5.5 : Fe_3O_4 NPs w/ w = 1 : 20, ratio Fe_3O_4 NPs : APTES w/w = 10 : 3, temperature 70 ^oC; pH 8.5; 5 hour reaction time. The obtained PLA-TPGS-Fe_3O_4-Dox-Cyanine 5.5 NPs have a spherical shape with an average size of 13.16 ± 2.16 nm, have good stability, and exhibit strong fluorescence, showing their potential applications in biomedicine. The combination of three components (Doxorubicin, Fe_3O_4, and Cyanine 5.5) in a multifunctional nano drug delivery system causes apoptosis on experimental cancer cell lines.

3. The *in vivo* distribution of the near-infrared fluorescent multifunctional nano drug delivery system has been evaluated on the CT26 colon tumor mouse model using optical bioimaging. The PLA-TPGS-Fe_3O_4-Dox-Cyanine 5.5 nanosystem is concentratedly distributed in the tumor effectively, reaching the highest level after 3 hours of injection, then cleared through the liver, spleen, and kidneys.

4. The ability to increase contrast in MRI imaging has been evaluated. Doxorubicin and Cyanine 5.5, when combined in the PLA-TPGS-Fe_3O_4-Dox-Cyanine 5.5 NPs, increase the T2 contrast effect of Fe_3O_4 NPs. Quantification of T2*-weighted MRI image signals using the %I0.25 method showed effective passive accumulation of the nanosystem at the tumor site, with the percentage of pixels below $I_{0.25}$ there was a significant difference ($p < 0.001$) between the control group (3.35 %) and the NPs treatment group (13.82 %).

5. The chemotherapeutic and hyperthermia effects of the multifunctional nano drug delivery system have been evaluated in an *in vivo* model. Chemotherapy effects after 72 hours of treatment with the multifunctional nano system PLA-TPGS-Fe_3O_4-Dox-Cyanine 5.5 were clearly observed by the bioluminescence method. Furthermore, the PLA-TPGS-Fe_3O_4-Dox-Cyanine 5.5 NPs demonstrated the effectiveness of synergistic effects when combining chemotherapy and magnetotherapy after 4 irradiations with a magnetic field intensity of 150 Oe and a frequency of 450 kHz for a period of 30 minutes.

On that basis, we propose the following recommendations:

1. Research on *in vivo* pharmacodynamic and pharmacokinetic properties of the near-infrared fluorecent multifunctional nano drug delivery systems.

2. Conduct further tests to develop the near-infrared fluorecent multifunctional nano drug delivery systems for application in cancer diagnosis and treatment.

NEW CONTRIBUTIONS OF THE PHD THESIS

1. We successfully fabricated a multifunctional nanodrug delivery system that simultaneously carries iron oxide nanoparticles from Fe_3O_4 NPs and Doxorubicin on a PLA-TPGS copolymer carrier.

2. We successfully fabricated a multifunctional nanodrug delivery system that simultaneously carries Fe_3O_4 NPs, Doxorubicin, and the near-infrared fluorescent agent Cyanine 5.5 on a PLA-TPGS copolymer carrier.

3. The *in vivo* distribution of the multifunctional drug delivery system in the mouse has been evaluated through the near-infrared fluorescence ability of PLA-TPGS-Fe_3O_4-Dox-Cyanine 5.5 NPs concentrate at the highest tumor location after 3 hours of injection. Organs such as the liver, spleen, and kidneys play a role in the metabolism and elimination of this nanosystem.

4. The nanosystem increases contrast in MRI imaging, the T2*-weighted MRI image signal quantified using the $\%I_{0.25}$ method shows effective passive accumulation of the nanosystem at the tumor site, with the percentage of pixels below $I_{0.25}$ there was a significant difference ($p < 0.001$) between the control group (3.35 %) and the NPs treatment group (13.82 %).

5. The chemotherapy effect of the multifunctional nano drug delivery system has been evaluated using the bioluminescence technique.

6. The hyperthermia effect of the multifunctional nano drug delivery system has been evaluated, showing a synergistic effect when combining chemotherapy and hyperthermia.